Temporal Evolution of a 3D Coronal Plasmoid, and its Impact on the Net Reconnection Flux Rate and Flare Ribbon Fine Structure

Marcel F. Corchado Albelo (CU Boulder, NSO, LASP), Maria D. Kazachenko (CU Boulder, NSO, LASP), Joel T. Dahlin (University of Maryland, NASA GSFC), Ryan J. French (LASP), Peter F. Wyper (Durham University), Georgios Chouliaras (Durham University)

Motivation

1. 3D magnetohydrodynamic simulations have suggested that the 3D resistive tearing mode instability can generate flare ribbon fine structures (Wyper & Pontin 2021 & Dahlin et al. 2025, Chouliaras et al. submitted).
2. Additionally, observational studies have shown that enhancements in the flare ribbon fronts widths (Naus et al. 2022) and multi-spatial scale features (Corchado Albelo 2026) temporally correlate with reconnection rate and hard X-Ray bursts, suggesting that the plasmoid instability plays a mayor role in particle acceleration and reconnection dynamics.

Goals

In this poster we present the analysis of 2 different plasmoids, from Dahlin et al. (2025), to highlight the effect of the plasmoids on the evolution of the flare ribbon's fine structures and reconnection flux rates.

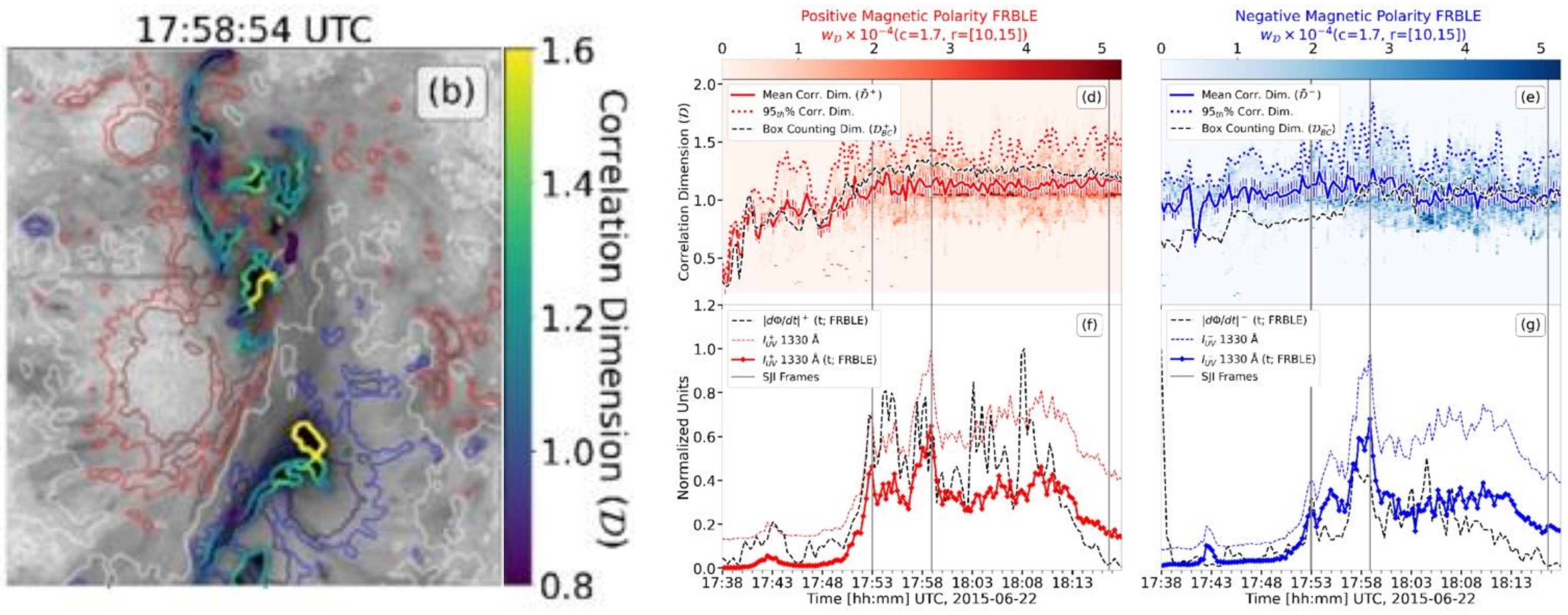

Figure 1. (a) IRIS 1330 Å observations of flare ribbon front highlighting morphological corrugations along the ribbon front boundaries (brighter colors). Alongside, the temporal evolution of the correlation dimension, and box counting dimension (d, e), IRIS 1330 Å emission and reconnection flux rates (f, g).

Geometry and Plasmoid Tracking Procedure

To track the evolution of the magnetic flux within the 3D plasmoid we simplify the complex geometry of the magnetic fields embedded within. Using the cylindrical model presented in Majeski et al. (2021) and the characterization techniques of Wang et al. (2024) we decompose the plasmoids magnetic field such that the axial component of cylindrical plasmoid is approximated by the longitudinal magnetic field (B_ϕ), and the in plane perpendicular components by the radial (B_r) and latitudinal (B_θ) magnetic field components. The tracking of the plasmoids is performed by following the local concentrations of the latitudinal magnetic field, while the core of the plasmoid is identified as the local minimum of the in plane perpendicular components.

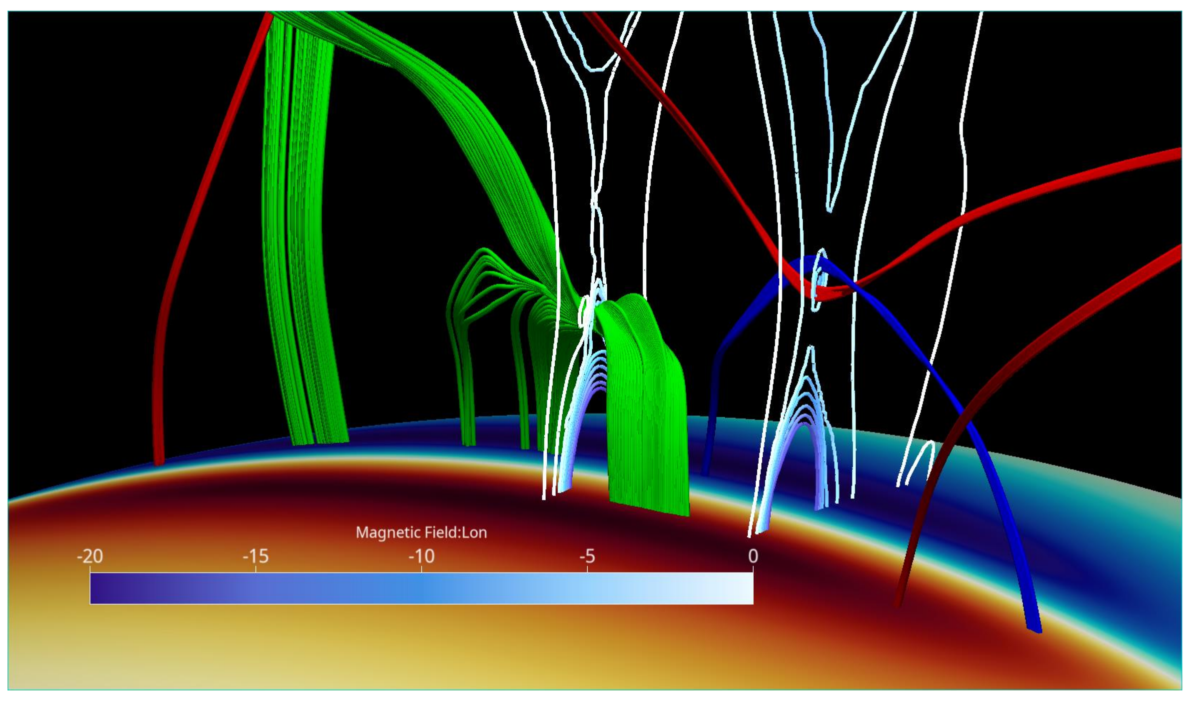

Figure 2. Magnetic field lines traced from the core structure of two 3D plasmoids. The green field lines trace a downward moving plasmoid. The blue and red lines trace an upward moving plasmoid.

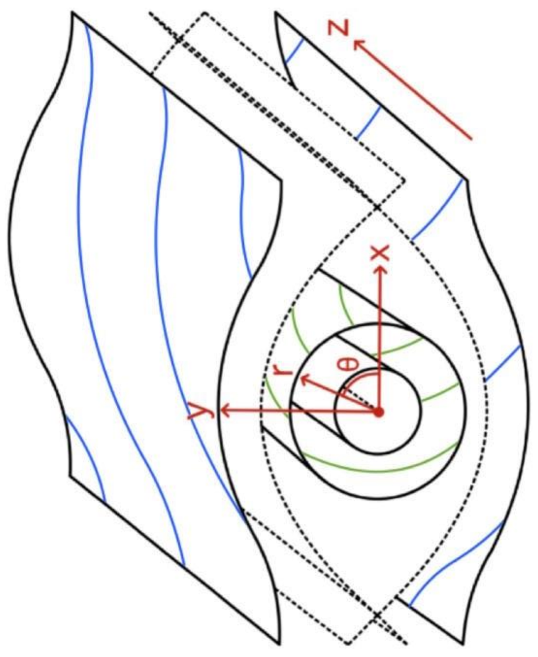

Figure 3. Simplified cylindrical geometry of a 3D plasmoid (Majeski et al. 2021).

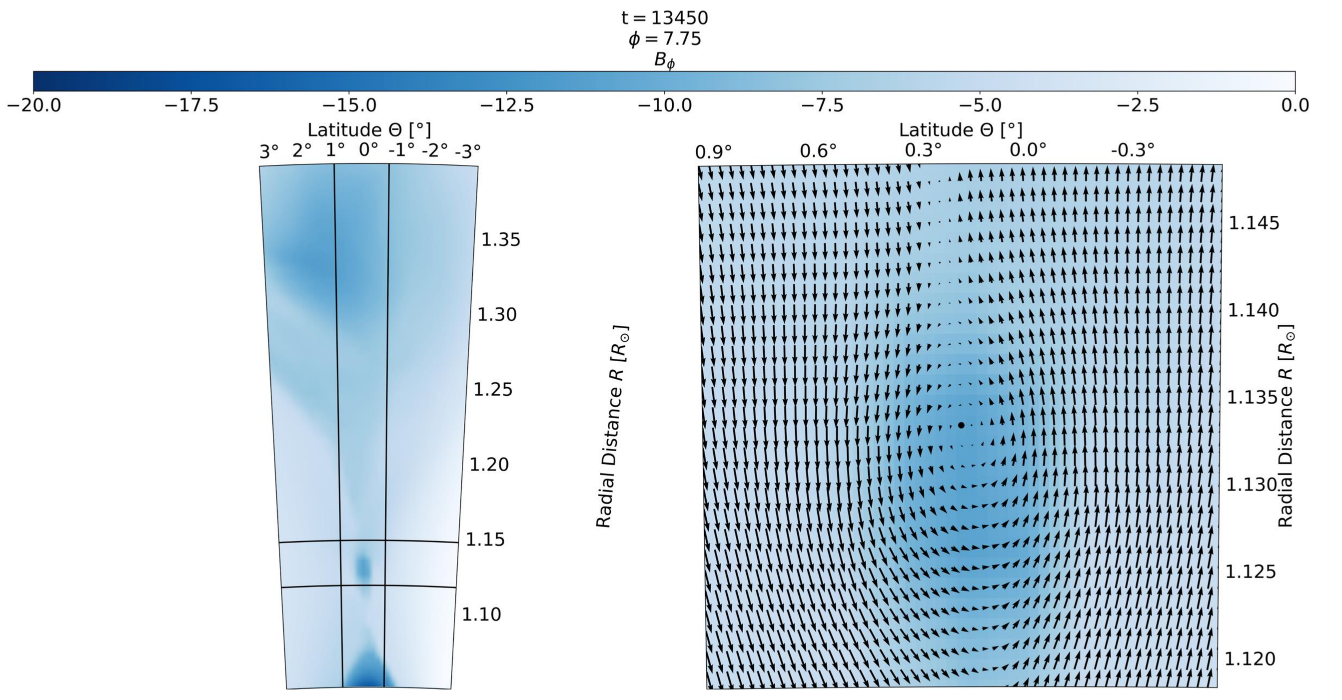

Figure 4. Plasmoid tracking based on concentrations of longitudinal magnetic field (serving as the axial component of the cylinder). The vector field shows the in plane perpendicular components of the magnetic field.

Mapping the Plasmoid Fluxes

By combining the plasmoid tracking procedure and the field line length maps (L-maps; Kazachenko et al. 2026) we can not only quantify the magnetic fluxes from the axial ($\Phi = \iint B_\phi \, dA$) and in plane azimuthal magnetic field ($\Psi = \iint B_\psi \, dA$) but also map these fluxes to their corresponding magnetic domains at the lower boundary of the simulation. Our results suggest that for both plasmoids, most of the axial flux is mapped to the inflow regions which is then converted into the dimming and flare ribbon regions, while most of the axial flux is distributed in the dimming regions.

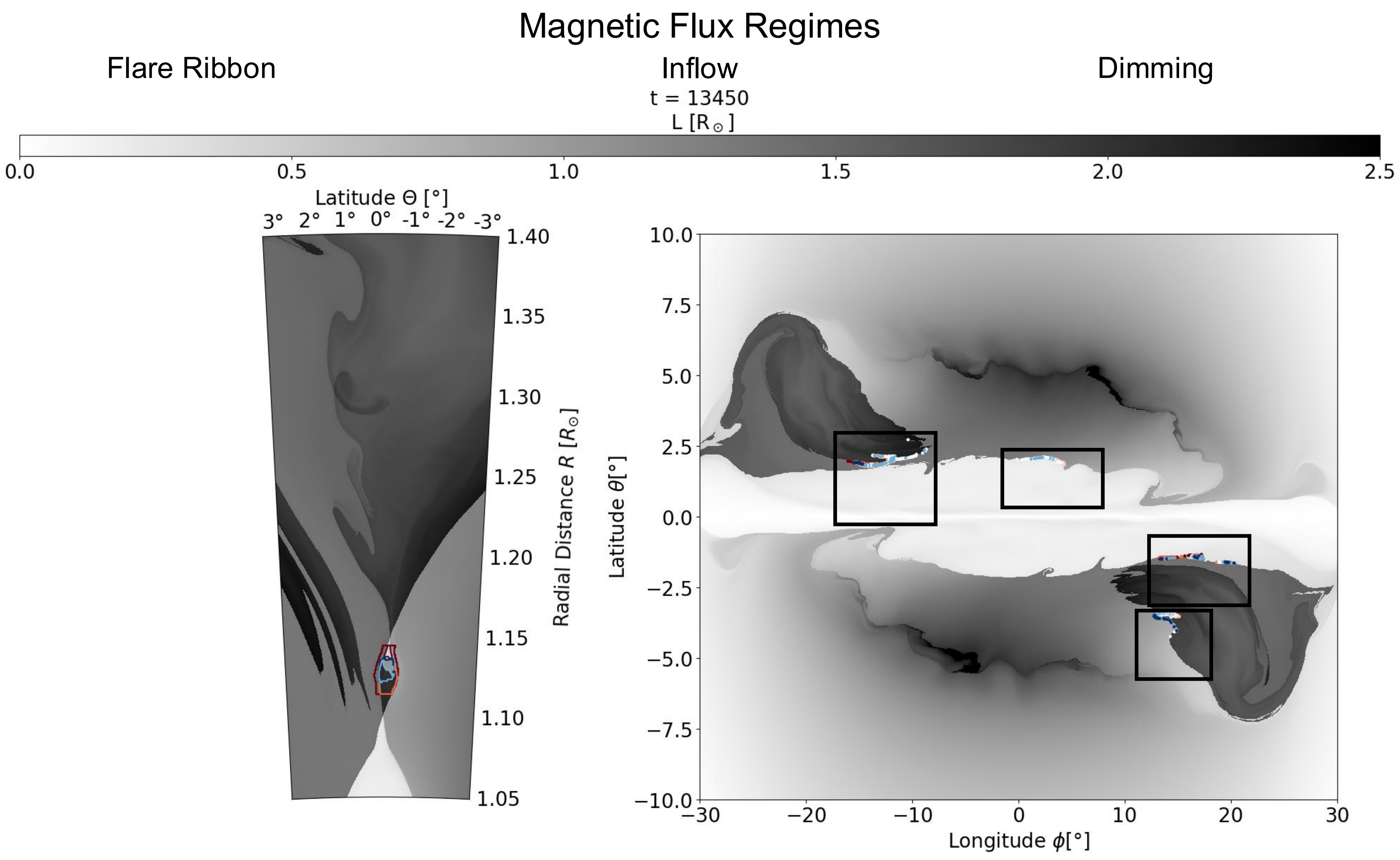

Figure 5. Vertical ($\phi = 7.75°$) and horizontal ($r = 1 \, R_\odot$) L-maps (Kazachenko et al. 2026). The contours highlight the magnetic field fluxes from the longitudinal component ($\Phi(B_\phi)$; blues), and the in-plane azimuthal magnetic field ($\Psi(B_\psi)$; reds). The same colors are used to highlight the footpoints of the magnetic fields enclosed within the plasmoids.

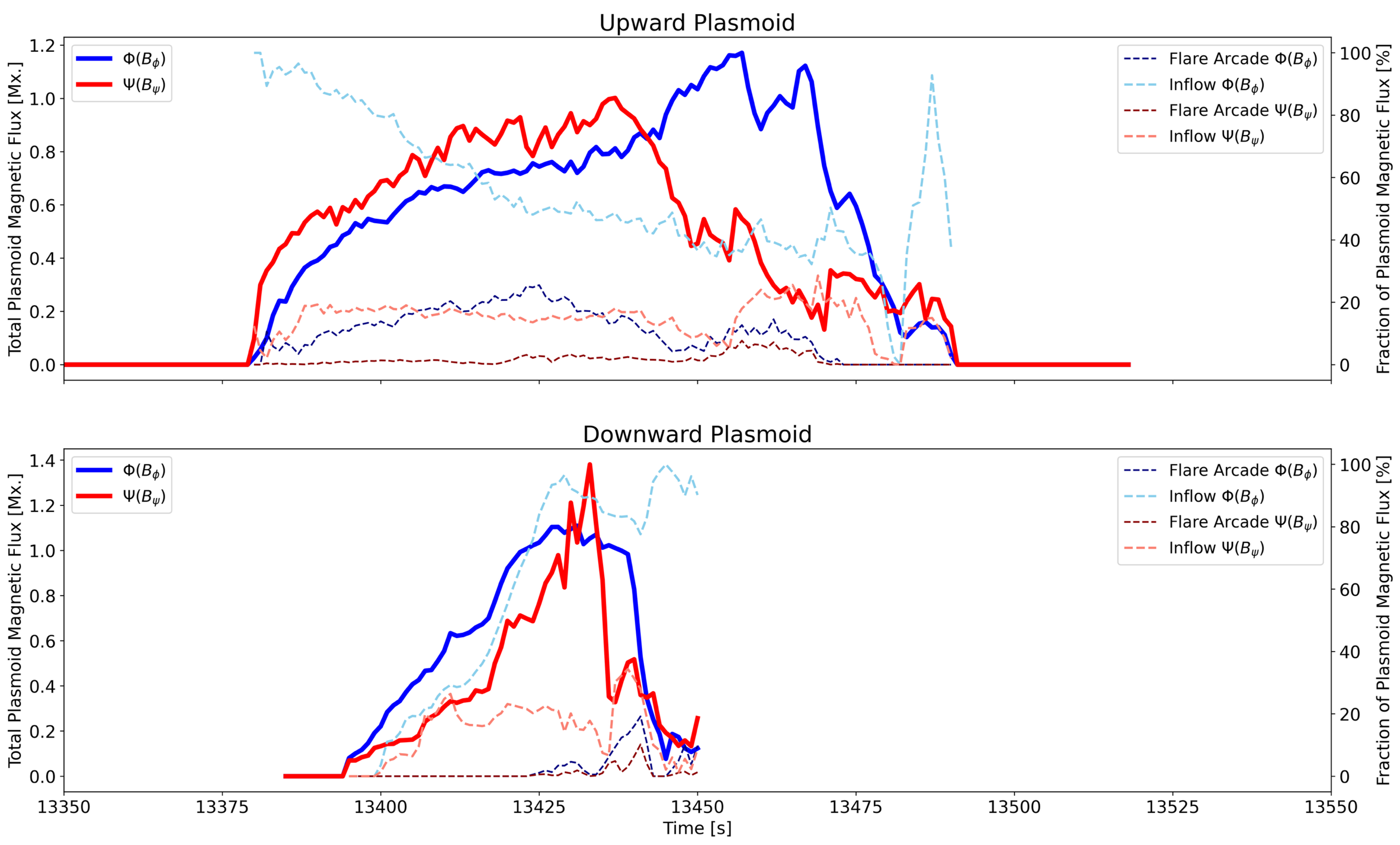

Figure 6. Temporal evolution of the magnetic fluxes of the plasmoids, and their decompositions based on their mapping properties.

Summary and Future Prospects

We find that by combing recent tracking and characterization techniques we can follow two plasmoids as they evolve and map their fluxes into flare ribbon and coronal diming regions. Furthermore, we observe that the plasmoids can enhance the conversion of inflow magnetic field into the flare ribbons, which can lead to bursty reconnection rates. More detailed decompositions are required to track the oblique tearing modes.

References